Available online at www.sciencedirect.com
SCIENCE DIRECT
Biochemical Pharmacology 69 (2005) 841–854
Biochemical Pharmacology
www.elsevier.com/locate/biochempharm

Contrasting the effects of nifedipine on subtypes of endogenous and recombinant T-type Ca^{2+} channels

Alexander Shcheglovitov[b,1], Tatiana Zhelay[b,1], Yulia Vitko[c], Vadim Osipenko[a], Edward Perez-Reyes[c], Platon Kostyuk[a], Yaroslav Shuba[a,b,*]

[a]*Bogomoletz Institute of Physiology, National Academy of Sciences of Ukraine, Bogomoletz St. 4, Kyiv-24, Ukraine*
[b]*International Center of Molecular Physiology, National Academy of Sciences of Ukraine, Bogomoletz St. 4, Kyiv-24, Ukraine*
[c]*Department of Pharmacology, University of Virginia, Charlottesville, VA 22908, USA*

Received 1 October 2004; accepted 30 November 2004

Abstract

There is evidence that nifedipine (Nif) – a dihydropyridine (DHP) Ca^{2+}-channel antagonist mostly known for its L-type-specific action – is capable of blocking low voltage-activated (LVA or T-type) Ca^{2+} channels as well. However, the discrimination by Nif of either various endogenous T-channel subtypes, evident from functional studies, or cloned $Ca_v3.1$, $Ca_v3.2$ and $Ca_v3.3$ T-channel α1 subunits have not been determined. Here, we investigated the effects of Nif on currents induced by $Ca_v3.1$, $Ca_v3.2$ and $Ca_v3.3$ expression in *Xenopus* oocytes or HEK-293 cells ($I_{\alpha 1G}$, $I_{\alpha 1H}$ and $I_{\alpha 1I}$, respectively) and two kinetically distinct, ''fast'' and ''slow'', LVA currents in thalamic neurons ($I_{LVA,f}$ and $I_{LVA,s}$). At voltages of the maximums of respective currents the drug most potently blocked $I_{\alpha 1H}$ (IC_{50} = 5 μM, max block 41%) followed by $I_{\alpha 1G}$ (IC_{50} = 109 μM, 23%) and $I_{\alpha 1I}$ (IC_{50} = 243 μM, 47%). The mechanism of blockade included interaction with $Ca_v3.1$, $Ca_v3.2$ and $Ca_v3.3$ open and inactivated states. Nif blocked thalamic $I_{LVA,f}$ and $I_{LVA,s}$ with nearly equal potency (IC_{50} = 22 μM and 28 μM, respectively), but with different maximal inhibition (81% and 51%, respectively). We conclude that $Ca_v3.2$ is the most sensitive to Nif, and that quantitative characteristics of drug action on T-type Ca^{2+} channels depend on cellular system they are expressed in. Some common features in the voltage- and state-dependence of Nif action on endogenous and recombinant currents together with previous data on T-channel α1 subunits mRNA expression patterns in the thalamus point to $Ca_v3.1$ and $Ca_v3.3$ as the major contributors to thalamic $I_{LVA,f}$ and $I_{LVA,s}$, respectively.

Keywords: Endogenous and cloned T-type Ca^{2+} channels; Nifedipine; Thalamic neurons; *Xenopus* oocytes

1. Introduction

Low voltage-activated (LVA) Ca^{2+} channels, otherwise known as T-type, lack specific ligands, which essentially impeded the progress in their molecular cloning compared to the high voltage-activated (HVA) counterparts. Moreover, native T-type Ca^{2+} channels display quite variable tissue-specific pharmacological sensitivity, suggesting the existence of their numerous functional subtypes. Recent cloning of three different T-channel pore-forming α1 subunits, α1G ($Ca_v3.1$), α1H ($Ca_v3.2$) and α1I ($Ca_v3.3$), through the use of in silico strategies [1–4] has provided a molecular basis for T-channel diversity. A logical extension of these findings is to correlate endogenous T-channel subtypes to specific cloned α1 subunits. In this respect determining tissue-specific expression of respective mRNAs or even proteins may not be sufficient, as their presence is no guarantee of functional channel. Therefore, comparison of functional properties of endogenous LVA channels and heterologously expressed α1 subunits is also required. Generally, the properties of endogenous channels depend not only on the nature of the primary pore-forming

Abbreviations: A_{max}, maximal percentage of inhibition; DMSO, dimethyl sulfoxide; HVA, high voltage-activated; IC_{50}, half-inhibitory concentration; $I_{\alpha 1G}$, current through heterologously expressed α1G ($Ca_v3.1$) subunit of low voltage-activated calcium channel; $I_{\alpha 1H}$, current through heterologously expressed α1H ($Ca_v3.2$) subunit of low voltage-activated calcium channel; $I_{\alpha 1I}$, current through heterologously expressed α1I ($Ca_v3.3$) subunit of low voltage-activated calcium channel; $I_{LVA,f}$, ''fast'' low voltage-activated current in thalamic neurons; $I_{LVA,s}$, ''slow'' thalamic low voltage-activated current; *I–V*, current–voltage relationship; *k*, slope factor; LD, laterodorsal; LVA, low voltage-activated; *p*, cooperativity coefficient; $V_{1/2}$, potential of half-maximal activation or inactivation; V_m, membrane potential

* Corresponding author. Tel.: +380 44 2562435; fax: +380 44 2536458.
E-mail address: yshuba@biph.kiev.ua (Y. Shuba).
[1] Contributed equally to this work.

0006-2952/$ – see front matter © 2004 Elsevier Inc. All rights reserved.
doi:10.1016/j.bcp.2004.11.024

α1 subunit but also on the presence of potential auxiliary subunits and/or other cell-specific regulatory factors. Thus, comparative studies of endogenous LVA currents in different cell types and the currents induced by heterologous expression of α1 subunits can be useful in providing information on both molecular organization of endogenous LVA channels as well as tissue-specific regulation of various α1 subunits.

The hallmark paper of Akaike et al. [5] gave rise to the notion that LVA Ca^{2+} channels in central neurons are more sensitive to the block by representatives of three classes of L-type Ca^{2+}-channel antagonists, phenylalkylamines (verapamil, D-600), dihydropyridines (DHPs—nifedipine, nicardipine) and benzothiazepines (diltiazem) as well as to the neuroleptic flunarizine compared to the ones in peripheral tissues [6]. We have recently identified two kinetically distinct, ''fast'' and ''slow'', endogenous LVA Ca^{2+}-channel subtypes in the neurons from rat laterodorsal (LD) thalamic nucleus [7–9]. In addition to the differences in the major biophysical properties, these channels were characterized by specific developmental pattern of the expression on neuronal surface and pharmacology. Interestingly, based on their sensitivity to nifedipine, flunarizine and La^{3+}, the pharmacology of only the ''fast'' thalamic LVA Ca^{2+} channel could be attributed to the ''central'' type, whereas the ''slow'' channel was characterized by distinct features of ''peripheral'' pharmacology manifested by the preference to amiloride and Ni^{2+} [7,9]. A limitation to these studies was that block was only studied at a single concentration of the agents, and dose–response relationships for the blockade of each of the channel subtype are still missing. In addition, there are no dose–response relationships for the action of these agents on the cloned T-channel α1 subunits either.

In the present study, we used pharmacological criteria, namely nifedipine sensitivity, in the attempt to distinguish LVA Ca^{2+} currents in thalamic neurons and shed some light on α1-subunit composition of underlying channels. To do so, we broke down the overall LVA Ca^{2+} current in isolated neurons from LD thalamic nucleus of 14–17-day-old rats onto two components based on the difference in the rate of inactivation and examined the effects of nifedipine on each of them. These were then compared to the effects of nifedipine on three subtypes of recombinant LVA Ca^{2+}-channel α1 subunits functionally expressed in *Xenopus* oocytes. Our results showed that $Ca_v3.2$ is the most sensitive to nifedipine, and that the mechanism of drug action is characterized by common for all subunits preferential interaction with activated and inactivated states. The dose–response relationships for the endogenous currents did not match any of those for the expressed ones, suggesting either the presence of yet unknown T-channel α1 subunit(s) or distinct regulation of pharmacological sensitivity of the existing subunits in thalamic neurons. Nevertheless, some common features in state-dependence of nifedipine action, together with previous reports on predominant $Ca_v3.1$ and $Ca_v3.3$ mRNA expression in the thalamus, allowed us to cautiously conclude that $Ca_v3.1$ and to a lesser extent $Ca_v3.2$ most likely contribute to the population of ''fast'' channels, whereas ''slow'' channels may be primarily composed of $Ca_v3.3$.

2. Materials and methods

2.1. Preparation of isolated thalamic neurons

Fourteen to seventeen days old rats were anesthetized with ether and decapitated. The brain was quickly removed from cranium and placed for 3–4 min in cold (4 °C) physiological saline 120 mM NaCl, 2.2 mM KCl, 2 mM $CaCl_2$, 1 mM $MgCl_2$, 24 mM $NaHCO_3$, 1.25 mM NaH_2PO_4, 15 mM glucose, pH 7.4 bubbled with carbogen (mixture of 95% O_2 and 5% CO_2). It was then separated into two hemispheres that were cut in the sagittal plane into a 300 μM thick slices using a razor blade. The slices that according to the rat brain stereotaxic atlas contained LD thalamic nucleus were selected and subjected to the enzymatic treatment with 20 mg/ml of pronase (Sigma) in physiological saline continuously bubbled with carbogen at room temperature for 30 min. After the treatment the slices were transferred into the bubbled enzyme-free saline. Isolated neurons were obtained by pipetting the slices. The suspension of the cells was transferred onto the cover slip and placed in the recording chamber.

2.2. Preparation of cRNA, isolation, maintenance and injection of Xenopus oocytes

Capped $Ca_v3.1$, $Ca_v3.2$ and $Ca_v3.3$ complementary RNA (cRNA) was prepared from linearized plasmid (pSP73 for $Ca_v3.3$, pGEM-HEA for $Ca_v3.1$ and $Ca_v3.2$) containing respective cDNA sequences using T7 mMessage mMachine in vitro transcription kit (Ambion).

Stage V and VI oocytes from adult female *Xenopus laevis* frogs were used for the recombinant T-type Ca^{2+}-channel expression. The procedures for oocyte isolation, maintenance and injection did not differ from those detailed elsewhere [10]. The volume of injected $Ca_v3.1$, $Ca_v3.2$ or $Ca_v3.3$ cRNA solution (0.2 μg/μl) was usually 50 nl per oocyte. The injection was performed using a semiautomatic nanoliter-range injector (Bibigon, Kyiv, Ukraine). Oocytes were used for the experiments 5 days after cRNA injection, since this time was required for maximal T-type Ca^{2+}-channel current expression (data not shown).

2.3. Electrophysiology and solutions

Macroscopic Ca^{2+}-channel currents in isolated thalamic neurons were measured using the whole-cell patch-clamp technique. To provide the best voltage-clamp performance,

we selected neurons with smallest spheroid or ovoid somata (about 20 μ in diameter) in their majority belonging to the local-circuit (according to Steriade and Llinas [11]) or associative (according to Batuev [12]) type although the presence of some small-size thalamocortical neurons also cannot be excluded. The cells in which there was evidence of the bad clamp (too steep descending branch of the *I–V*, inadequate current waveform) were discarded from the analysis. The extracellular recording solution 10 mM $SrCl_2$, 150 mM choline-Cl, 1 mM $MgCl_2$, 10 mM HEPES, pH 7.4 (adjusted with tetraethylammonium (TEA) hydroxide), as well as intracellular pipette solution 120 mM Cs(OH), 10 mM CsCl, 10 mM HEPES, 10 mM EGTA, pH 7.3 (adjusted with H_3PO_4) were composed such as to suppress all transmembrane currents except the current through LVA Ca^{2+} channels. In most of the cells HVA Ca^{2+} current was not large to begin with, however, to minimize its contribution we usually started recording 5 min after establishing whole-cell configuration which given the lack of any metabolic supplements in the intracellular solution was sufficient time for complete HVA current rundown.

Membrane currents in the oocytes were recorded using a conventional double-microelectrode voltage-clamp technique as described before [10]. ''Voltage recording'' and ''current passing'' microelectrodes were pulled from borosilicate glass and had resistance of ~3 MΩ and ~1 MΩ, respectively, when filled with 3 M KCl. To reduce contamination of $Ca_v3.1$-, $Ca_v3.2$- and $Ca_v3.3$-induced currents by the oocyte's endogenous Ca^{2+}-dependent Cl^- current, all measurements were conducted in Cl^--free, methanesulfonate-substituted extracellular solution with Ba^{2+} as a charge carrier: 66 mM Na(OH); 2 mM K(OH); 10 mM $Ba(OH)_2$; 10 mM HEPES; pH 7.4 (adjusted with methanesulfonic acid). Experiments on non-injected oocytes showed that under such conditions endogenous currents are minimal.

Membrane currents in HEK-293 cells were recorded using the whole-cell ruptured patch-clamp technique. The methods used to prepare and record from stably transfected HEK-293 cells expressing $Ca_v3.1$, $Ca_v3.2$, and $Ca_v3.3$ have been described previously [13]. Whole cell Ca^{2+} currents were recorded using the following external solution: 5 mM $CaCl_2$; 155 mM TEA-Cl; and 10 mM HEPES; pH adjusted to 7.4 with TEA-OH. The internal pipette solution contained the following: 125 mM CsCl; 10 mM EGTA; 2 mM $CaCl_2$; 1 mM $MgCl_2$; 4 mM Mg-ATP; 0.3 mM Na_3GTP; and 10 mM HEPES; pH adjusted to 7.2 with CsOH.

Appropriate concentrations of nifedipine (Sigma) were added to the experimental solutions from 100 mM stock dissolved in DMSO. Control experiments have shown that 0.5%, 0.1% and 0.2% DMSO coming with the highest nifedipine concentrations of 500 μM, 100 μM and 200 μM used in oocytes, HEK-293 cells and thalamic neurons, respectively, by itself did not affect the currents of interest in the respective cell system. Special precautions were taken at all stages to minimize exposure of nifedipine-containing solutions to light.

2.4. Data analysis and statistics

Currents were measured in each cell in control and after successive applications of the nifedipine at increasing concentrations. The percentage of inhibition was tabulated for each cell and then averaged. The data points were presented as mean ± S.E.M. (standard error of the mean). We used Student's *t*-test to determine statistical significance of the results: $p < 0.05$ was considered to be statistically significant. Data analysis was performed using pCLAMP 8 (Axon Instr., Foster City, CA, USA) and Origin 6.0 (Microcal, Northampton, MA, USA) software.

The total low voltage-activated current in thalamic neurons (I_{LVA}) was dissected into ''fast'' ($I_{LVA,f}$) and ''slow'' ($I_{LVA,s}$) components using exponential stripping procedure, as detailed in our previous works [8,9] and summarized in Fig. 2A. Briefly, the total I_{LVA} was presented in semi-logarithmic scale (Fig. 2A, right panel, filled circles), and the late linear portion of this current was fit with linear function, which was then interpolated to the beginning of depolarization (time ''0''). The slope of this function provided the time constant (τ_{in}) of $I_{LVA,s}$ exponential decay, whose reconstruction is presented in Fig. 2A (left panel, black circles). Point-by-point subtraction of $I_{LVA,s}$ from total I_{LVA} allowed derivation of $I_{LVA,f}$ (Fig. 2A, left panel, open circles). Presentation of $I_{LVA,f}$ in semi-logarithmic scale (Fig. 2A, right panel, open circles) and fitting with linear function yielded τ_{in} of its decay. The amplitudes of both $I_{LVA,f}$ and $I_{LVA,s}$ were measured at a time-to-peak of the total I_{LVA} (Fig. 2A, left panel, dashed line).

3. Results

3.1. Concentration-dependence of nifedipine action

Fig. 1 shows representative Ba^{2+} currents through α1G, α1H and α1I ($I_{α1G}$, $I_{α1H}$ and $I_{α1I}$) expressed in *Xenopus* oocytes and Fig. 2 endogenous Sr^{2+}-carried LVA currents in freshly isolated LD thalamic neurons. We selected Ba^{2+} as a charge carrier through heterologously expressed T-channel α1 subunits because it minimizes contribution of oocyte's endogenous Ca^{2+}-dependent currents without taking special precautions (i.e., BAPTA injection) for their reduction, and Sr^{2+} as a charge carrier through the native neuronal LVA channels as it provides the most favorable relation between the currents carried by their ''fast'' ($I_{LVA,f}$) and ''slow'' ($I_{LVA,s}$) subtypes [8]. α1G-, α1H- and α1I-carried currents in stably transfected HEK-293 cells were recorded using Ca^{2+} as charge carrier, because it provided the highest stability of the recordings.

Applications of nifedipine in the 1–500 μM concentration range suppressed the currents carried by all three

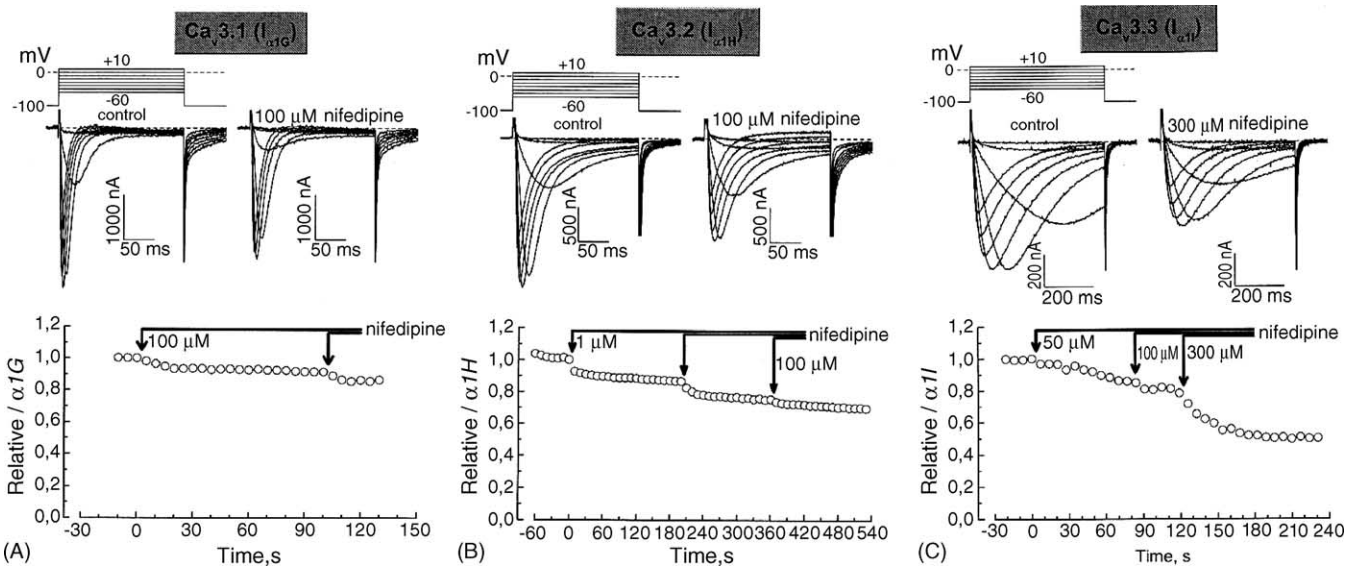

Fig. 1. Effects of nifedipine on Ba^{2+} currents induced in *Xenopus* oocytes by expression of recombinant T-type Ca^{2+}-channel α1 subunits. (A) Tracings of the control currents and currents in the presence of 100 μM nifedipine at different step potentials recorded in a representative $Ca_v3.1$-expressing oocyte ($I_{\alpha 1G}$, upper panel). Lower panel shows the time course of peak $I_{\alpha 1G}$ decreases at −20 mV in response to the specified nifedipine concentrations. Pulse protocol used to activate currents is shown above the control recordings. (B and C) Same as in (A), but for nifedipine action on $I_{\alpha 1H}$ in $Ca_v3.2$-expressing oocyte and $I_{\alpha 1I}$ in $Ca_v3.3$-expressing oocyte, respectively.

T-channel α1 subunits (Fig. 1A–C). The steady level of inhibition developed within about 30 s following drug application irrespective of current nature (Fig. 1A–C), however, the effective ranges of drug concentrations were different. Nifedipine blocked $I_{\alpha 1H}$ at 1–100 μM whereas 10-times higher concentrations were required to produce comparable $I_{\alpha 1G}$ and $I_{\alpha 1I}$ inhibition.

Nifedipine also suppressed the total LVA current in thalamic neurons (I_{LVA}, Fig. 2B, upper panels). In order to distinguish drug effects on the subtypes of endogenous thalamic LVA channels, we dissected the total I_{LVA} into $I_{LVA,f}$ and $I_{LVA,s}$ components before and after drug administering using exponential stripping procedure (Fig. 2A, see also Section 2 and Refs. [8,9]). Lower panel of Fig. 2B shows the time course of the changes of peak $I_{LVA,f}$ and $I_{LVA,s}$ (extracted from total I_{LVA}) during consecutive applications of 50 μM and 100 μM nifedipine. It is evident that the relative decrease of $I_{LVA,s}$ in response to the identical drug concentrations was about two-fold smaller than that of $I_{LVA,f}$, suggesting lower nifedipine sensitivity of the "slow" channels compared to the "fast" ones.

Fig. 1 and Fig. 2B show that the action of nifedipine on the expressed $I_{\alpha 1G}$, $I_{\alpha 1H}$ and $I_{\alpha 1I}$ and endogenous $I_{LVA,f}$ and $I_{LVA,s}$ were concentration-dependent. In order to quantify this concentration-dependency, we measured dose–response relationships for each current at test potentials (V_m) corresponding to the maximums of their respective *I–V*s (V_m = −20 mV for $I_{\alpha 1G}$ and $I_{\alpha 1H}$, V_m = −10 mV for $I_{\alpha 1I}$, and V_m = −30 mV for $I_{LVA,f}$ and $I_{LVA,s}$) and fitted them with a Hill equation (Fig. 3). Fitting procedures provided such parameters of nifedipine action as the percentage of maximal blockade at infinitely high drug concentration, A_{max}, the concentration of half-maximal blockade, IC_{50}, characterizing the affinity of drug binding, and Hill (cooperativity) coefficient, *p*. It should be noted that, as evident from dose–response relationships of Fig. 3, nifedipine was able to produce only partial, although variable in size, inhibition of all types of T-type Ca^{2+}-channel currents studied. Unfortunately, because of poor nifedipine solubility it was virtually impossible to prepare solutions with more than 300 μM nifedipine, which in most cases was insufficient to produce reliably saturable block. Therefore, in defining the level of maximal blockade we had to rely on fitting of experimental data points with Hill equation.

Nifedipine inhibited $I_{\alpha 1H}$ and $I_{\alpha 1I}$ by nearly the same maximal value (A_{max}) of 41% and 45%, respectively, but $I_{\alpha 1G}$ by only 23%. However, the affinity of the blockade was the highest for $I_{\alpha 1H}$ (IC_{50} = 5 μM), followed by about 20-times lower affinity for $I_{\alpha 1G}$ (IC_{50} = 109 μM) and about 50-times lower for $I_{\alpha 1H}$ (IC_{50} = 243 μM). The cooperativity coefficient for the blockade of $I_{\alpha 1H}$ and $I_{\alpha 1G}$ agreed well with p = 1, suggesting one-to-one binding, but was considerably higher (p = 3.7) for $I_{\alpha 1I}$ suggesting positive cooperativity in nifedipine action on α1I.

Evaluation of the dose–response relationships for the nifedipine action on endogenous thalamic $I_{LVA,f}$ and $I_{LVA,s}$ (at V_m = −30 mV) showed that the drug blocks $I_{LVA,f}$ almost 1.6-fold stronger (A_{max} = 81%), and with slightly higher affinity (IC_{50} = 22 μM) compared to $I_{LVA,s}$ (A_{max} = 51%, IC_{50} = 28 μM), whereas cooperativity coefficient for each current could be satisfactorily taken as p = 1. Thus, in terms of the affinity of nifedipine-induced blockade endogenous thalamic LVA channel subtypes stand somewhere in between recombinant α1H and α1G.

In order to verify, if the difference in the permeating ion (i.e., Ba^{2+} in oocytes versus Sr^{2+} in neurons) is responsible

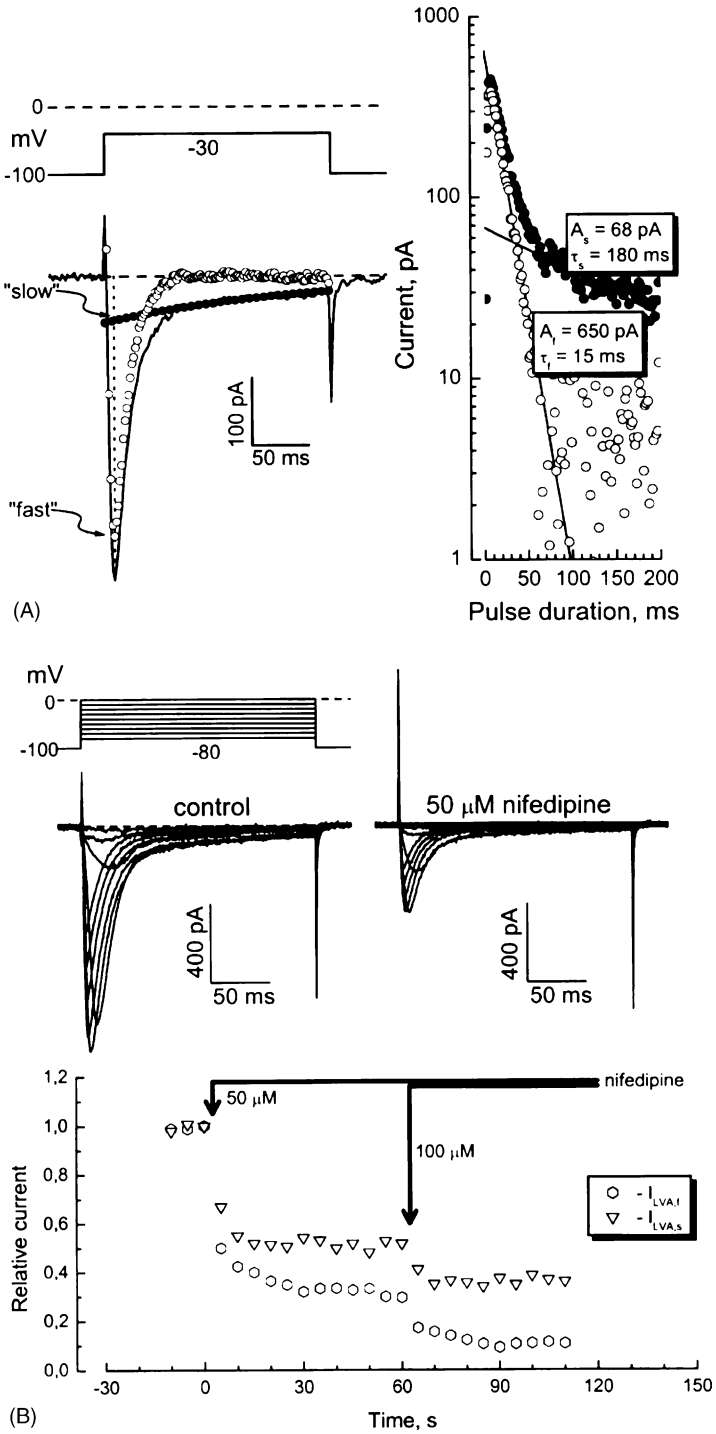

Fig. 2. Effects of nifedipine on the subtypes of LVA Ca^{2+} channels in isolated thalamic neurons. (A) The procedure of $I_{LVA,f}$ and $I_{LVA,s}$ isolation. Left-hand panel, the recording of the total I_{LVA} (continuous line) in response to the depicted voltage-clamp protocol with superimposed $I_{LVA,s}$ (filled circles) $I_{LVA,f}$ (open circles); the dashed vertical line indicates the time to I_{LVA} peak at which the amplitudes of the "fast" and "slow" currents (pointed by arrowhead lines) were measured. Right-hand panel, semi-logarithmic plot of I_{LVA} (filled circles) with superimposed line representing the fit of the slow phase of I_{LVA} decay with a linear function, the slope of which provides the time constant $\tau_s = 180$ ms of $I_{LVA,s}$ exponential decay; open circles represent semi-logarithmic plot of $I_{LVA,f}$ obtained following subtraction of $I_{LVA,s}$ recreated based on the determined τ_s from the total I_{LVA}; the slope of the line fitted to the open circles provides the time constant $\tau_f = 15$ ms of $I_{LVA,f}$ exponential decay. (B) Upper panels, representative tracings of the total Sr^{2+}-carried currents (I_{LVA}) at different step potentials under control conditions (left) and in the presence of 50 μM nifedipine (right). Lower panel, time courses of the changes of the "fast" ($I_{LVA,f}$, open diamonds) and "slow" ($I_{LVA,s}$, open triangles) LVA currents at −30 mV in response to the specified nifedipine concentrations.

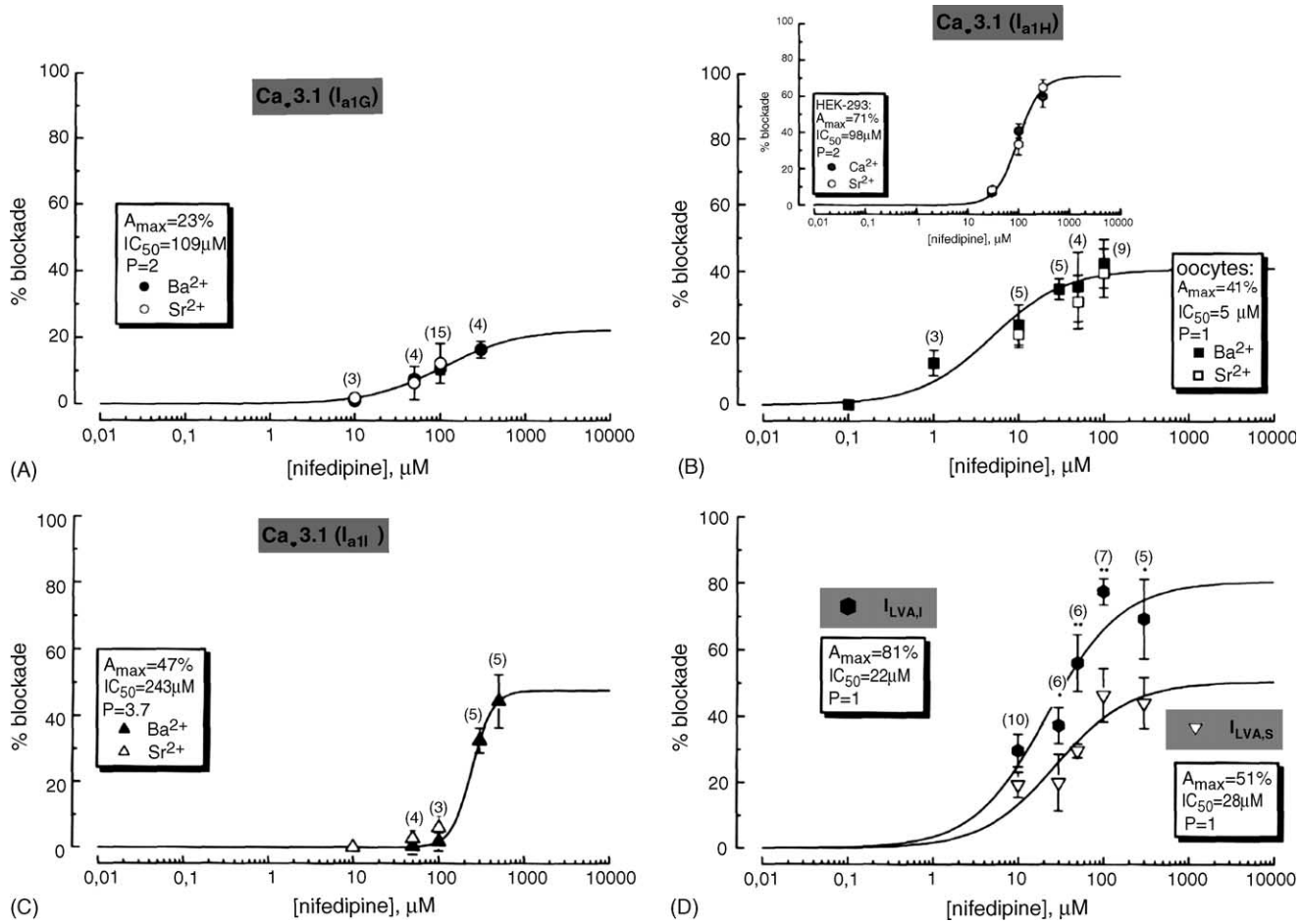

Fig. 3. Concentration dependence of nifedipine action on recombinant T-type Ca^{2+}-channel α1 subunits expressed in *Xenopus* oocytes and endogenous T-channel subtypes in thalamic neurons. (A) Dose–response relationship for the nifedipine action on $I_{\alpha 1G}$ in $Ca_v3.1$-expressing oocytes for Ba^{2+} (filled symbols, mean ± S.E.M., n is indicated in parenthesis above each data point) and Sr^{2+} (open symbols, mean ± S.E.M., $n = 4$–6); smooth line represents the best fit of experimental data points for Ba^{2+} with Hill equation: % blockade = $100(1 - I_{drug}/I_o) = A_{max}(1 - 1/(1+([drug]/IC_{50})^p))$, where I_{drug} and I_o are the currents in the presence and in the absence of the drug, [drug] is drug concentration, IC_{50} is drug concentration for half-maximal block, p is cooperativity coefficient and $A_{max} = 100(1 - I_{min}/I_o)$ is the percentage of maximal blockade (i.e., I_{min} is the current at infinitely high [drug]); the parameters of the fit are shown on the plot. (B and C) Same as in (A), but for nifedipine action on $I_{\alpha 1H}$ in $Ca_v3.2$-expressing oocytes (B) and $I_{\alpha 1I}$ in $Ca_v3.3$-expressing oocytes (C); inset in (B) represents similar dose–response relationship for $Ca_v3.2$ expressed in HEK-293 cells with Ca^{2+} (gray symbols) and Sr^{2+} (open symbols). (D) Analogous dose–response relationship for $I_{LVA,f}$ (filled symbols) and $I_{LVA,s}$ (open symbols) in thalamic neurons; significantly different values of the blockade of these two currents are marked by "*" or "**" for $P < 0.05$ and $P < 0.01$, respectively.

for the lack of apparent similarity in dose–response relationships of nifedipine action on recombinant and endogenous T-channels, we applied three nifedipine concentrations, 10 μM, 50 μM and 100 μM, on α1G-, α1H- and α1I-expressing oocytes when using 10 mM Sr^{2+} instead of 10 mM Ba^{2+} as a charge carrier. Despite contaminating outward currents were higher in the presence of Sr^{2+} compared to Ba^{2+}, this did not preclude correct measurements of Sr^{2+} peak currents. Moreover, the experimental data points for Sr^{2+} currents inhibition ($n = 4$–6 for each data point) fall reasonably well onto dose–response relationships for the nifedipine action on Ba^{2+} currents (Fig. 3A–C, open symbols), suggesting that the nature of permeating ion does not contribute to any appreciable extent to the observed differences in the blockade of recombinant and endogenous T-type Ca^{2+} channels.

Furthermore, we have also compared dose–response relationships for nifedipine action on Ca^{2+} and Sr^{2+} currents through $Ca_v3.2$ stably expressed in HEK-293 cells (Fig. 3B, inset). Although the parameters of $Ca_v3.2$ blockade in HEK-293 cells ($IC_{50} = 98$ μM, $A_{max} = 71\%$, and $p = 2$) appeared to be very different from those in oocytes (i.e., $IC_{50} = 5$ μM, $A_{max} = 41\%$, and $p = 1$, Fig. 3B), nevertheless, there was no apparent difference in the blockade of Ca^{2+} and Sr^{2+} currents, consistent with major role of cell-specific environment, rather than the nature of charge carrier in defining T-channel pharmacological sensitivity.

3.2. State-dependence of nifedipine action

To gain insight into possible mechanisms of nifedipine blocking action on recombinant T-channel α1 subunits and endogenous thalamic LVA Ca^{2+}-channel subtypes, we

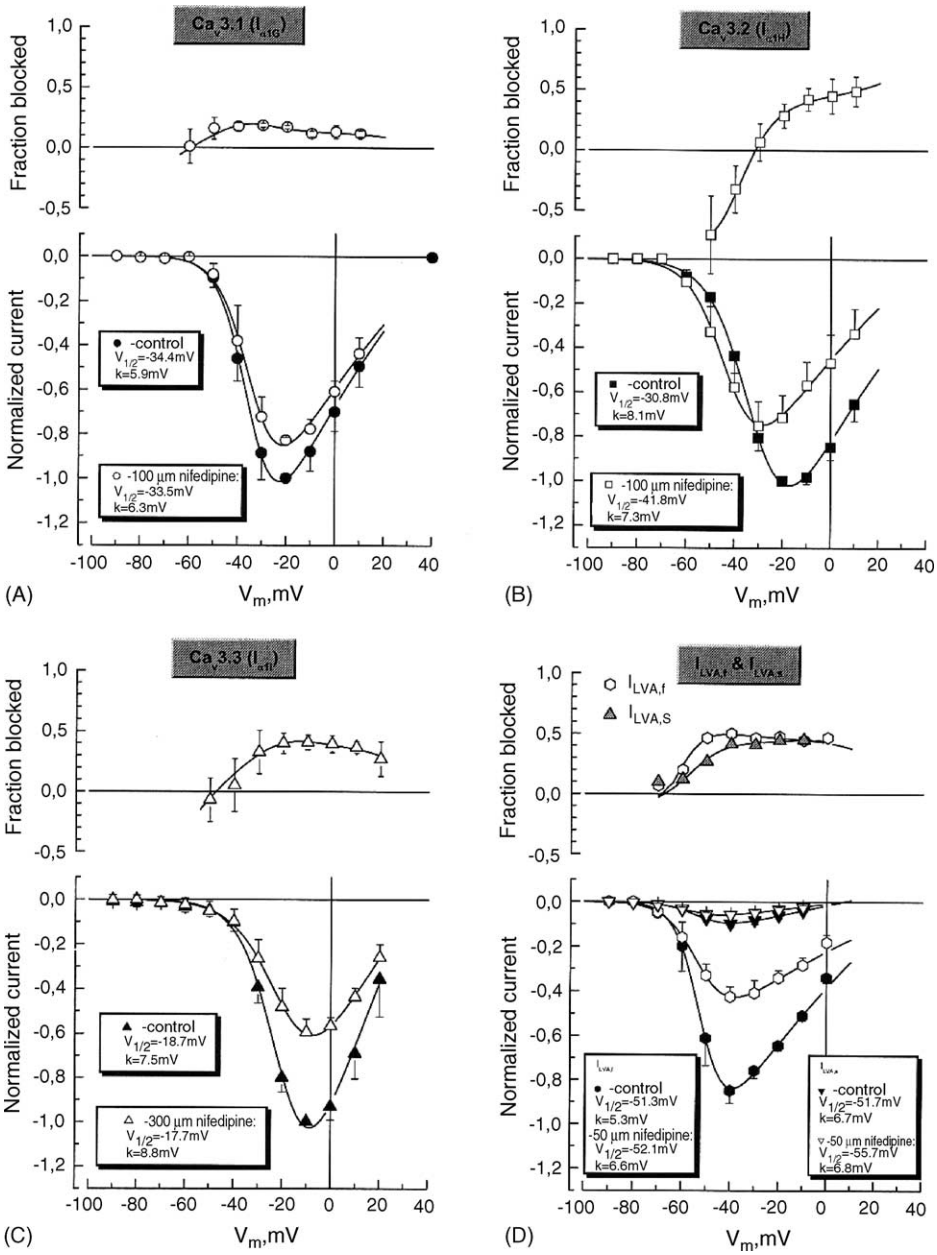

Fig. 4. Voltage-dependence of nifedipine action on recombinant T-type Ca^{2+}-channel α1 subunits expressed in *Xenopus* oocytes and endogenous T-channel subtypes in thalamic neurons. (A) Lower panel, normalized and averaged *I–V* relationships (mean ± S.E.M., $n = 10$) for $I_{\alpha 1G}$ in $Ca_v3.1$-expressing oocytes under control conditions (filled symbols) and following exposure to the specified nifedipine concentration (open symbols). The *I–V*s for each oocyte were normalized to the control $I_{\alpha 1G}$ amplitude at −20 mV and then averaged. Smooth lines represent the best fit of the data points with the product of Boltzmann and Goldman–Hodgkin–Katz functions; the derived parameters of steady-state activation—half activation potential, $V_{1/2}$, and slope factor, k, are shown. Upper panel, the plot of the fraction of $I_{\alpha 1G}$ blocked at each voltage derived from data points of *I–V*s (symbols) and respective fitting curves (smooth line). (B–D) Same as in (A), but for nifedipine action on $I_{\alpha 1H}$ in $Ca_v3.2$-expressing oocytes (B), $I_{\alpha 1I}$ in $Ca_v3.3$-expressing oocytes (C), $I_{LVA,f}$ and $I_{LVA,s}$ in thalamic neurons (D); $I_{\alpha 1H}$ and $I_{\alpha 1I}$ *I–V*s were normalized to the control amplitudes at −20 mV and −10 mV, respectively, whereas $I_{LVA,f}$ and $I_{LVA,s}$ *I–V*s were normalized to the control amplitude of the total I_{LVA} at −40 mV.

measured the voltage-dependence of block, the time-dependence of block during voltage-clamp pulse as well as compared drug-induced alterations in steady-state inactivation properties of the respective currents.

Fig. 4 shows normalized and averaged *I–V* relationships for the peak $I_{\alpha 1G}$, $I_{\alpha 1H}$, $I_{\alpha 1I}$, $I_{LVA,f}$ and $I_{LVA,s}$ in control and in the presence of specified nifedipine concentrations. Derivation of the fraction of current inhibition at each voltage from respective *I–V*s (Fig. 4) showed that the blockade of $I_{\alpha 1G}$ increased from the values slightly below zero (suggesting potentiation instead of inhibition) at potentials close to the threshold for current activation to the maximum of about 20% around −20 mV, which corresponds to the *I–V* peak, and then declined somewhat at higher depolarizations (upper panel of Fig. 4A). Generally similar voltage-dependence was observed for $I_{\alpha 1I}$ (upper panel of Fig. 4C), whereas for $I_{\alpha 1H}$ current potentiation at voltages corresponding to the negative slope of *I–V* was

much more pronounced and, in addition, inhibition at voltages above *I–V* peak showed no obvious signs of decline (upper panel of Fig. 4B).

Fit of $I_{\alpha 1G}$, $I_{\alpha 1H}$ and $I_{\alpha 1I}$ *I–V* relationships in the absence and in the presence of nifedipine with the product of Boltzmann and Goldman–Hodgkin–Katz equations has shown that the drug produced no significant change in the half-maximal $I_{\alpha 1G}$ and $I_{\alpha 1I}$ steady-state activation potentials, $V_{1/2}$ (lower panels of Fig. 4A and C), but caused about a 10 mV hyperpolarizing shift in $V_{1/2}$ for $I_{\alpha 1H}$ (upper panel of Fig. 4B). The slope factors, *k*, of steady-state activations of all currents were little affected by nifedipine. Thus, the strong potentiating effect of nifedipine on $I_{\alpha 1H}$ at negative voltages can be explained by the pronounced drug-induced shift of $I_{\alpha 1H}$ steady-state activation in the hyperpolarizing direction.

As *I–V* relationships were constructed from peak currents at each voltage step, which are little affected by inactivation, the voltage-dependencies of nifedipine action described thus far indicate that the drug acts as a weak agonist on α1G and α1I resting/closed states and turns into a blocker as channels activate. The same apparently holds true for α1H, although in this case nifedipine in addition causes a hyperpolarizing shift of steady-state activation may be due to influence on S4 voltage sensor.

Voltage-dependences of nifedipine-induced blockade of endogenous thalamic $I_{LVA,f}$ and $I_{LVA,s}$ (upper panel of Fig. 4D) most resembled those of $I_{\alpha 1G}$ and $I_{\alpha 1I}$, respectively, if one also considers current's kinetics criteria (i.e., $I_{LVA,f}$ and $I_{\alpha 1G}$ are fast currents and $I_{LVA,s}$ and $I_{\alpha 1I}$ are the slow ones). As evident from the *I–V*s, nifedipine action $I_{LVA,f}$ and $I_{LVA,s}$ were not accompanied by changes in $V_{1/2}$ or *k* values for their activation (lower panel of Fig. 4D), which is also similar to what has been observed for $I_{\alpha 1G}$ and $I_{\alpha 1I}$ (lower panel of Fig. 4A and C).

To examine the dependence of nifedipine action on recombinant T-channels inactivation, we used two experimental protocols. First, we derived the time-courses of drug action during a depolarizing pulse and compared them with the current's waveforms, and, second, we measured

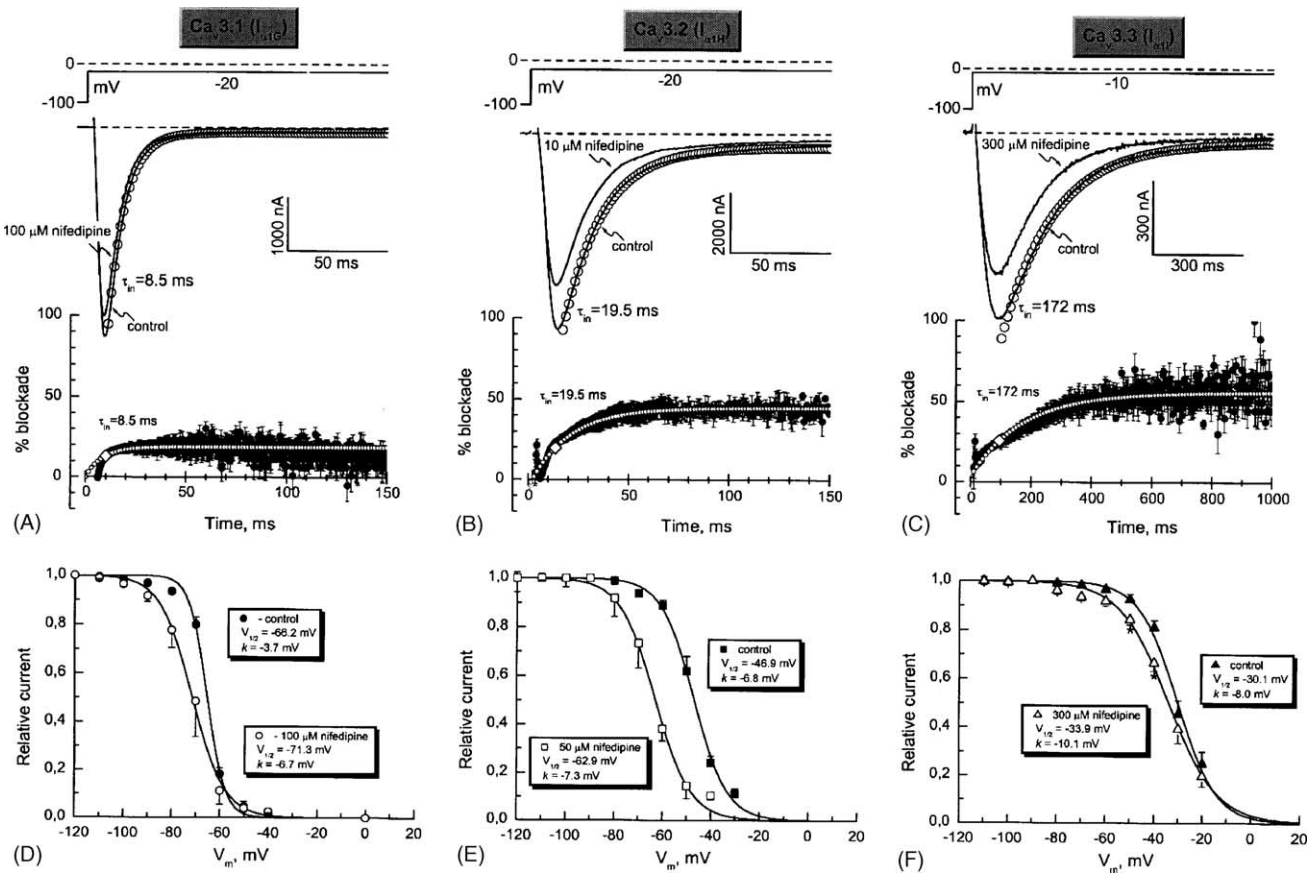

Fig. 5. Time-dependence of nifedipine action on recombinant T-type Ca^{2+}-channel α1 subunits during depolarization pulse. (A) Upper panel, representative $I_{\alpha 1G}$ traces in $Ca_v3.1$-expressing oocyte before (control) and after exposure to the specified nifedipine concentration; voltage-clamp protocol is shown above the traces; open circles represent mono-exponential fit of control current inactivation with specified time constant (τ_{in}). Lower panel, the average time-course of $I_{\alpha 1G}$ blockade (filled circles, mean ± S.E.M., $n = 8$) during voltage-clamp pulse with superimposed mono-exponential function (open circles) having the same time constant as current inactivation; the diamond marks the position of the peak current. (B and C) Same as in (A), but for nifedipine action on $I_{\alpha 1H}$ in $Ca_v3.2$-expressing oocyte (B) and $I_{\alpha 1I}$ in $Ca_v3.3$-expressing oocyte (C). (D) Steady-state inactivation dependencies (mean ± S.E.M., n =4–7) of the control $I_{\alpha 1G}$ (filled symbols) and $I_{\alpha 1G}$ in the presence of specified nifedipine concentration (open symbols) and their fits with a Boltzmann equation (smooth lines); the parameters of each fit – half inactivation potential, $V_{1/2}$, and slope factor, *k* – are presented. (E and F) Same as in (D), but for $I_{\alpha 1H}$ in $Ca_v3.2$-expressing oocytes (E) and $I_{\alpha 1I}$ in $Ca_v3.3$-expressing oocyte (F); "*"on F denotes significant difference with $P < 0.05$. See text for details.

the steady-state inactivation curves using standard procedure: conditioning depolarizing pre-pulses (durations of 0.6 s for the fast inactivating $I_{\alpha 1G}$ and $I_{\alpha 1H}$, and 2 s for slowly inactivating $I_{\alpha 1I}$) to different voltages followed by the test pulse to −20 mV.

The lower panels of Fig. 5A–C, show that as depolarization progressed the $I_{\alpha 1G}$, $I_{\alpha 1H}$ and $I_{\alpha 1I}$ blockade increased from close to zero values at the beginning of depolarization to the maximal plateau levels with the time-courses identical to those of respective current inactivation, indicating preferential nifedipine action on α1G, α1H and α1I inactivated states. Consistent with progressive inhibition as channels enter inactivated state, the apparent rate of currents inactivation in the presence of drug accelerated. For instance, for $I_{\alpha 1G}$, $I_{\alpha 1H}$ and $I_{\alpha 1I}$ traces presented in Fig. 5A–C the time constant of inactivation (τ_{in}) decreased from 8.5 ms to 7 ms, from 19.5 ms to 16 ms and from 172 ms to 140 ms, respectively.

Nifedipine also hyperpolarized $I_{\alpha 1G}$, $I_{\alpha 1H}$ and $I_{\alpha 1I}$ steady-state inactivation by ∼5 mV, ∼17 mV and ∼4 mV, respectively (Fig. 5D–F). Such shifts suggest that in the presence of nifedipine a smaller current compared to the control can be evoked from more depolarized holding potentials, which drive channels to inactivation. These results are consistent with enhanced drug binding to α1G, α1H and α1I inactivated states. This is especially true for α1H, for which nifedipine induced the largest negative shift of steady-state inactivation. Interestingly, the negative shift of α1H steady-state inactivation was basically parallel (Fig. 5E), while for α1G and α1I it was accompanied by notable change in the slope factor, k (Fig. 5D and F), suggesting alterations in the effective charge of the gating particles.

Unfortunately, the presence of capacity transients and the likelihood of the changes in the speed of voltage clamp during drug administering introduces a degree of uncertainty in determining the starting level of the blockade at depolarization onset, which would be indicative of the mode of drug action on resting/closed state, as well as its progression during the phase of rapid channel's activation. However, the deviations of the actual blockade from pure inactivation time-course before the peak current is reached (Fig. 5A–C, lower panels) suggest drug interaction with α1G, α1H and α1I activated states as well.

Fig. 6A shows that the extent of nifedipine-induced blockade of the total thalamic I_{LVA} reasonably follows inactivation time course only during first 50 ms of depolarization, after which it essentially declines. Such biphasic inhibition reflects the presence of two current components, $I_{LVA,f}$ and $I_{LVA,s}$, with different nifedipine sensitivity: the more sensitive $I_{LVA,f}$ is the major contributor to the total current at early times (<50 ms), whereas

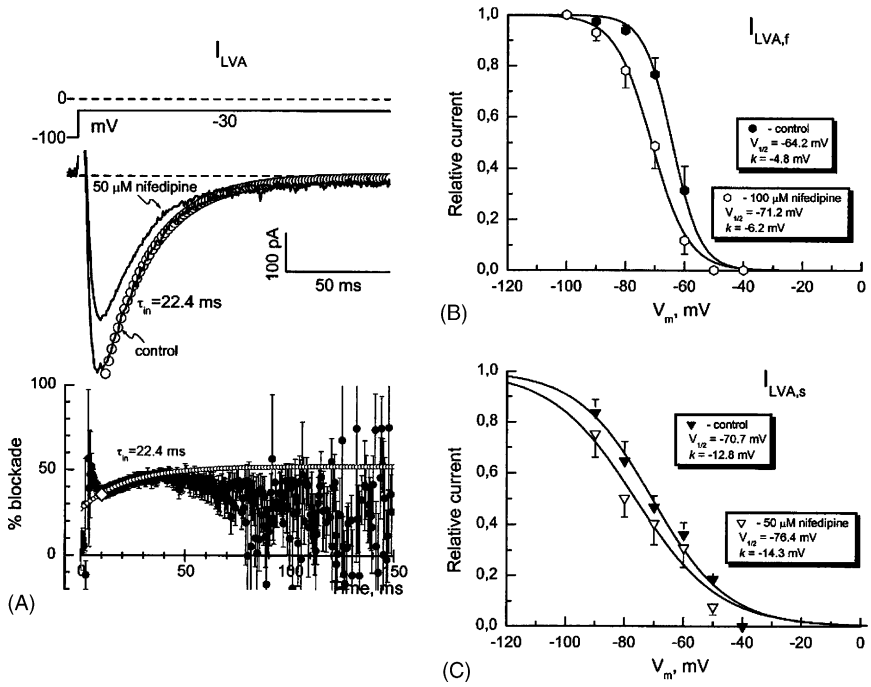

Fig. 6. Time-dependence of nifedipine action on endogenous thalamic LVA currents during depolarizing pulse. (A) Upper panel, representative I_{LVA} traces in thalamic neuron before (control) and after exposure to 50 μM nifedipine; voltage-clamp protocol is shown above the traces; open circles represent mono-exponential fit of control current inactivation with specified time constant (τ_{in}). Lower panel, the average time-course of I_{LVA} blockade (filled circles, mean ± S.E.M., n = 10) during voltage-clamp pulse with superimposed mono-exponential function (open circles) having the same time constant as current inactivation. (B) Steady-state inactivation dependencies (mean ± S.E.M., n = 4–7) of the control $I_{LVA,f}$ (filled symbols) and $I_{LVA,f}$ in the presence of 100 μM nifedipine (open symbols), smooth curves represent the best fit of experimental data points with a Boltzmann equation (smooth lines); the parameters of each fit – half inactivation potential, $V_{1/2}$, and slope factor, k – are presented on the graph. (C) Same as in (B), but for $I_{LVA,s}$.

less sensitive $I_{LVA,s}$ becomes the dominant one at later times. In addition, despite considerable scatter of inhibition values at the very beginning of depolarization due to the presence of capacity transients and probable variations in the speed of voltage-clamp, adequate fit with inactivation time-course is only possible from some non-zero initial level (Fig. 6A, lower panel), suggesting that $I_{LVA,f}$ is first rapidly blocked during activation. The possibility that $I_{LVA,f}$ might already be blocked in the resting/closed state is highly unlikely, as it contradicts the established voltage-dependence of nifedipine action on $I_{LVA,f}$ (Fig. 4D, upper panel). Nifedipine also produced about a 6–7 mV hyperpolarizing shift of $I_{LVA,f}$ and $I_{LVA,s}$ steady-state inactivation curves (Fig. 6B), further supporting the notion of drug interaction with "fast" and "slow" channels inactivated states.

3.3. Comparison to other expression system

To examine whether or not the major features of nifedipine action on recombinant T-type Ca^{2+}-channel α1 subunits are dependent on the expression system, we repeated key experiments in HEK-293 cells stably expressing α1G, α1H and α1I. The results obtained in HEK-293 cells were qualitatively similar to those obtained in oocytes, although a number of quantitative differences were noted. Fig. 7 exemplifies the analysis of drug action on α1G expressed in HEK-293 cells. Similar to the oocyte expression system, the blockade of $I\alpha_{1G}$ in HEK-293 cells increased from values below zero at threshold potentials for current activation to its maximum at depolarizations of complete channel activation (upper panel of Fig. 7A), consistent with weak agonistic action on channel's rest-

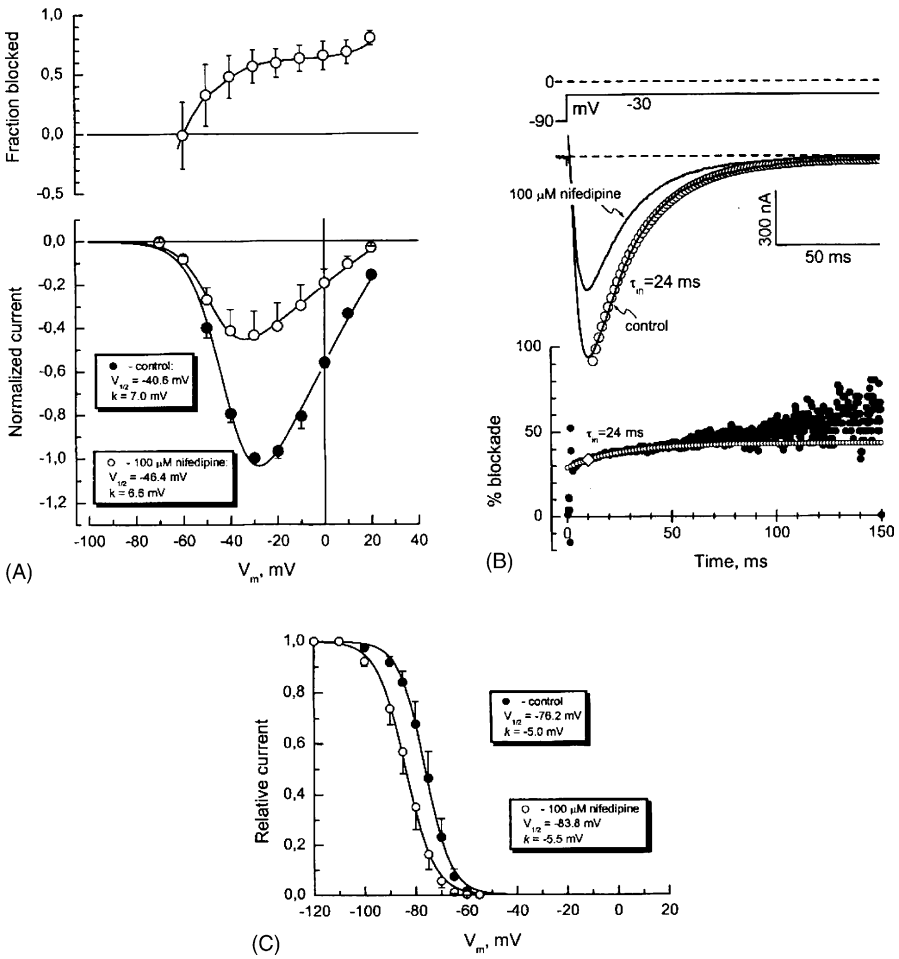

Fig. 7. Effects of nifedipine on $Ca_v3.1$ expressed in HEK-293 cells. (A) Lower panel, normalized and averaged *I–V* relationships (mean ± S.E.M., $n = 6$) of $I_{\alpha 1G}$ in $Ca_v3.1$-expressing HEK-293 cells under control conditions (filled symbols) and following exposure to 100 μM nifedipine (open symbols). The *I–Vs* for each cell were normalized to the control $I_{\alpha 1G}$ amplitude at −30 mV and then averaged. Smooth lines represent the best fit of the data points with the product of Boltzmann and Goldman–Hodgkin–Katz functions; the derived parameters of steady-state activation—half activation potential, $V_{1/2}$, and slope factor, k, are shown. Upper panel, the plot of the fraction of $I_{\alpha 1G}$ blocked at each voltage derived from data points of *I–Vs* (symbols) and respective fitting curves (smooth line). (B) Upper panel, representative $I_{\alpha 1G}$ traces in $Ca_v3.1$-expressing HEK-293 cell before (control) and after exposure to 100 μM nifedipine; voltage-clamp protocol is shown above the traces; open circles represent mono-exponential fit of control current inactivation with specified time constant (τ_{in}). Lower panel, the time-course of $I_{\alpha 1G}$ blockade (filled circles) during voltage-clamp pulse with superimposed mono-exponential function (open circles) having the same time constant as current inactivation; the diamond marks the position of the peak current. (C) Steady-state inactivation dependencies (mean ± S.E.M., $n = 6$) of the control $I_{\alpha 1G}$ (filled symbols) and $I_{\alpha 1G}$ in the presence of 100 μM nifedipine (open symbols) and their fits with a Boltzmann equation (smooth lines); the parameters of each fit – half inactivation potential, $V_{1/2}$, and slope factor, k – are presented.

ing/closed state and blocking action on activated state. However, the maximal $I_{\alpha 1G}$ inhibition achieved in HEK-293 cells with 100 μM nifedipine was higher than in oocytes, i.e., ~60% (upper panel of Fig. 7A) versus ~20% (upper panel of Fig. 4A), suggesting higher potency of drug action. In addition, nifedipine caused about a 6 mV hyperpolarizing shift in α1G half maximal steady-state activation (i.e., $V_{1/2}$, lower panel of Fig. 7A), which was not apparent in the oocyte's system.

Despite generally following current inactivation time-course during depolarization, the higher fraction of $I_{\alpha 1G}$ blockade in HEK-293 cells occurred immediately after depolarization onset even before full current activation (lower panel of Fig. 7B). These results suggest very rapid drug binding to channel's activated state. In this respect, α1G expressed in HEK-293 cells is similar to the endogenous "fast" LVA channel in thalamic neurons. Nifedipine also caused about an 8 mV hyperpolarizing shifted of $I_{\alpha 1G}$ steady-state inactivation in HEK-293 cells consistent with drug interaction with α1G inactivated state as well.

Nifedipine action on α1H and α1I expressed in HEK-293 cells was also characterized by the enhanced blockade at voltages corresponding to the higher steady-state activation of the channels, and by a negative shift of their steady-state inactivation (data not shown), as was documented in *Xenopus* oocytes. Thus, one can conclude that the major features of nifedipine action on recombinant T-channel α1 subunits are invariant to the expression system, although cell-specific environment is capable of modulating their sensitivity. This may introduce a degree of uncertainty when one tries to correlate recombinant α1 subunits to the endogenous LVA currents in various cell types based on pharmacological criteria.

4. Discussion

In the present study, we report on the following major findings: (1) the DHP Ca^{2+}-channel antagonist nifedipine most effectively blocks $Ca_v3.2$ followed by $Ca_v3.1$ and $Ca_v3.3$; (2) the action of nifedipine includes interaction with $Ca_v3.1$, $Ca_v3.2$ and $Ca_v3.3$ activated and inactivated states; (3) the major characteristics of state-dependence of nifedipine action are invariant of the expression system, although quantitative differences are observed; (4) the potency and efficacy of the drug action are cell-specific; (5) endogenous thalamic $Ca_v3.1$ and to a lesser extent $Ca_v3.2$ most likely contribute to the population of "fast" subtype of LVA channels in thalamic neurons, whereas their "slow" subtype is mainly comprised of $Ca_v3.3$.

4.1. DHP effects on LVA Ca^{2+} currents in native tissues

The notion that classical L-type Ca^{2+} channel antagonists including DHPs are also capable of blocking LVA Ca^{2+} channels, especially in central neurons, originates from the hallmark study of Akaike et al. [5] in freshly isolated hypothalamic neurons. In that study IC_{50}'s between 3.5 μM and 7 μM were found for the blocking action of such DHP representatives as nicardipine, nifedipine and nimodipine. Micromolar concentrations of nicardipine, amlodipine and nilvadipine were reported to block LVA current also in hippocampal neurons with the potency comparable to their effects on L-type current [14–16]. Subsequently, the evidence has accumulated that some DHP derivatives may act on LVA Ca^{2+} channels in other preparations as well. For instance, nicardipine but not nifedipine inhibited T-type Ca^{2+} current in mouse DRG neurons (93% versus <20% inhibition at 5 μM [17]), niguldipine has been shown to suppress equally strong T- and L-type currents in atrial cardiomyocytes (IC_{50}~0.18 μM [18]), and niguldipine, nicardipine, nimodipine, nifedipine blocked with high potency (IC_{50}-s 0.24 μM, 2.5 μM, 9.8 μM and 39 μM, respectively) T-type Ca^{2+} current in NG108-15 neuroblastoma-glioma cell line [19]. In most reported cases the action of DHP derivatives was time-, voltage- and use-dependent.

The quite broad spectrum of T-type Ca^{2+} channels blocking potencies found for DHP representatives in various preparations may suggest the importance of drug chemical structure for the optimal drug-channel interaction [20], although it may also indicate diverse cell-specific patterns of T-channel α1 subunits expression. Indeed, nifedipine sensitivity has been used as one of the major criteria for the functional identification of "fast" and "slow" subpopulations of LVA channels in thalamic neurons [7]. However, despite the importance of the whole issue for the full appreciation of pharmacological profile of various DHPs as well as for the correlation of cell-specific endogenous T-channel currents to the cloned α1 subunits, comparative studies of the action of DHP representatives on either heterologously expressed α1 subunits or the subtypes of endogenous channels have not been performed.

4.2. The effects of nifedipine on recombinant T-channel α1 subunits

We focused on nifedipine as it had been used in our previous studies to separate subtypes of endogenous T-type Ca^{2+} channels in thalamic neurons [7,9] and because it remains one of the most popular antihypertensive drugs. Our results show that of the three recombinant T-channel α1 subunits expressed in *Xenopus* oocytes, nifedipine most potently blocked $Ca_v3.2$, which is expressed more widely in peripheral tissues, such as kidney, liver and heart, than in the brain [2]. For instance, the IC_{50} of 5 μM that we have found for $Ca_v3.2$ is very similar to the $IC_{50} = 5.7$ μM reported for the inhibitory action of the currently most widely prescribed antihypertensive DHP agent, amlodipine, on endogenous T-type Ca^{2+} channels in guinea pig

atrial myocytes [21]. Interestingly, although endogenous T-type Ca^{2+} channels in atrial myocytes are apparently primarily composed of $Ca_v3.2$, amlodipine was shown to block heterologously expressed $Ca_v3.2$ in HEK293 cells with an IC_{50} of only 31 μM [21], suggesting that cellular environment is important in determining drug binding. In contrast to the complete block produced by amlodipine, we find that nifedipine could only produce partial block of $Ca_v3.2$ currents in either oocytes or HEK-293 cells. These results suggest that alterations in DHP structure can lead to dramatic changes in both the potency and efficacy of their interaction with Ca_v3 channels, supporting their use in drug development [22]. Moreover, we find that partial block by nifedipine is characteristic of all T-type Ca^{2+}-channel currents studied in all cell systems used. As nifedipine action is associated with the decrease of open channel probability [23], then partial block is most likely explained by inability of the drug to reduce T-channel open probability to "0" at any concentration.

Our results show that nifedipine is ~20- and ~50-times less potent in inhibiting $Ca_v3.1$ and $Ca_v3.3$ expressed in *Xenopus* oocytes compared to $Ca_v3.2$. Basically identical to our IC_{50} of about 100 μM was also found for nifedipine action on $Ca_v3.1$ expressed in tsa-201 cells [22]. Given that $Ca_v3.1$ and $Ca_v3.3$ are the dominant subunits in the brain [1,3,24,25], such low affinities is difficult to reconcile not only with IC_{50}-s in micromolar range for the nifedipine inhibitory action on LVA currents in central neurons reported in literature (e.g., [5,7]), but also with somewhat higher IC_{50}~20–30 μM obtained herein for the two subtypes, "fast" and "slow", of endogenous LVA currents in thalamic neurons. Moreover, we find that nifedipine is able to produce only partial $Ca_v3.1$, $Ca_v3.2$ and $Ca_v3.3$ blockade, whereas the studies in native cells imply full blockade of endogenous LVA currents.

The blocking action of nifedipine is characterized by preferred interaction with $Ca_v3.1$, $Ca_v3.2$ and $Ca_v3.3$ activated and inactivated states, whereas in the resting/closed state the drug can even act as an agonist. However, the affinity and rate constants of drug interaction with various states seems to depend not only on specific subunits, but also on the cellular system they are expressed in, as evidenced, for instance, by different time-dependence of $Ca_v3.1$ inhibition during depolarization pulses in oocytes and HEK-293 cells as well as by strongly divergent dose-dependence of nifedipine action on $Ca_v3.2$ expressed in oocytes (IC_{50} = 5 μM, A_{max} = 41%, p = 1) and HEK-293 cells (IC_{50} = 5 μM, A_{max} = 41%, p = 1). The reasons for such differences are not yet clear, but may be related to the specifics in T-channels regulation, post-translational processing, accessory subunit composition in various cell models and/or to structural or compositional features of membrane lipid bilayer, which may strongly influence channel interaction with such lipophilic drug as nifedipine.

The DHP receptor site in the highly DHP-sensitive L-type Ca^{2+} channel-forming α1C subunit includes nine critical amino acids belonging to IIIS5, IIIS6 and IVS6 transmembrane segments, which upon transfer to non-L-type HVA Ca^{2+} channel α1 subunits can confer high DHP sensitivity [26–28]. In the non-L-type HVA Ca^{2+} channel α1 subunits only four of these amino acids are conserved, which allows them to exhibit, although much lower and variable, but measurable sensitivity to the wide range of DHP derivatives [29]. Such variability implies the existence of other determinants for DHPs action as well. This is even more likely for T-type Ca^{2+}-channel α1 subunits, for which all residues in equivalent positions are different from "classical" L-type DHP binding site, although they are 100% conserved within all members of T-channel family. Taken together with our results on different potencies and quantitative characteristics of nifedipine action on $Ca_v3.1$, $Ca_v3.2$ and $Ca_v3.3$ this rules out the role of "classical" DHP site in the mechanism of such action, but rather suggests the existence of alternative site(s) with non-identical amino acid composition.

4.3. α1-subunit composition of endogenous thalamic LVA Ca^{2+}-channel subtypes

Because all three recombinant T-channel α1 subunits exhibit similar state-dependence of nifedipine action, but different affinities depending on the expression system, the correlation of specific α1 subunits to endogenous channel subtypes become quite challenging. This is especially true for the population of "fast" thalamic channels, which according to pure kinetic criteria may potentially rely on two, $Ca_v3.1$ and $Ca_v3.2$, subunits. Nevertheless, comparison of the state-dependencies of the blockade mostly implicates $Ca_v3.1$, as the major contributor to the "fast" channels. Indeed, (i) nifedipine did not produce any shift in $I_{\alpha 1G}$ and $I_{LVA,f}$ steady-state activation, but substantially shifted negatively steady-state activation of $I_{\alpha 1H}$, (ii) nifedipine rapidly blocked $I_{\alpha 1G}$ (expressed in HEK-293 cells) and $I_{LVA,f}$ during their activation phases, which was not as evident for $I_{\alpha 1H}$, and finally, (iii) nifedipine-induced a negative shift of $I_{\alpha 1G}$ and $I_{LVA,f}$ steady-state inactivation that was comparable in size and notably smaller than that of $I_{\alpha 1H}$. The principal role of endogenous thalamic $Ca_v3.1$ "fast" channels is also supported by in situ hybridization studies in adult rats, which showed dominant $Ca_v3.1$ mRNA expression in thalamic relay nuclei with $Ca_v3.2$ mRNA levels being below detection threshold [24,25,30]. However, considering that expression of endogenous thalamic LVA Ca^{2+}-channel subtypes is strongly age-dependent [7], one cannot exclude a higher contribution of $Ca_v3.2$ at early developmental stages. It is also possible that the cells from the $Ca_v3.2$-rich reticular nucleus could contaminate cell preparations used in our experiments.

It should be noted that in our experiments the current associated with the activation of the "slow" subtype of thalamic LVA Ca^{2+} channels (i.e., $I_{LVA,s}$) was isolated from

the total current solely based on kinetic considerations. Given the small size of $I_{LVA,s}$, such procedure cannot guarantee lack of its contamination by the currents carried through the channels with ''fast'' kinetics. Nevertheless, taken together our data suggest that $Ca_v3.3$ is responsible for $I_{LVA,s}$ currents. This notion is also supported by the observation that both $I_{LVA,s}$ and $I_{\alpha 1I}$ are characterized by relatively slow kinetics, and a big window current (e.g., [9,31]), as well as share some similarities in state-dependence of nifedipine action. In addition, $Ca_v3.3$ mRNA has been shown to be present in most of the thalamic nuclei even in adult rat [24]. Almost a 10-fold higher affinity of nifedipine blocking action which we find for $I_{LVA,s}$ compared to $I_{\alpha 1I}$ can be explained by cell-specific regulation of channel pharmacology or the presence of another, yet unknown T-channel $\alpha 1$-subunit with slow kinetics.

One cannot also exclude the contribution of $Ca_v2.3$ (rbE-II or $\alpha 1E$), which represents R-type Ca^{2+}-channel $\alpha 1$ subunit, to the thalamic $I_{LVA,s}$. Indeed, kinetic, voltage-dependent and pharmacological properties – in particular high Ni^{2+} sensitivity – of $Ca_v2.3$ are such that upon initial cloning it was even mistakenly suggested as a T-type channel $\alpha 1$ subunit [32]. $Ca_v2.3$ is expressed in thalamus, particularly in intralaminar, parafascicular and reticular nuclei [32,33], however, the developmental pattern of its expression in this brain structure is not known. In addition, endogenous R-type current in many preparations as well as heterologously expressed $Ca_v2.3$ is completely insensitive to nifedipine and other DHPs (e.g., [29]).

4.4. The role of T-channel α1 subunits in thalamic neuronal physiology

In our recent study [9], we used the bulk of available data on biophysical properties, developmental expression, and surface localization of LVA channels in the neurons from LD thalamic nucleus to conclude that the ''slow'' subtype was most probably involved in Ca^{2+} signaling required for the outgrowth of the neurites and formation of the neuronal networks, whereas ''fast'' subtype participated in the generation of low-threshold Ca^{2+} spikes and bursting activity known to be a distinguishing feature of thalamic neurons [11]. Although this conclusion may be mainly related to the population of local-circuit thalamic neurons, which we believe were the primary object of our study, it is still important for highlighting developmental and signaling aspects in physiological significance of ''slow'' and ''fast'' LVA channels, respectively. Our present pharmacological data on nifedipine actions, which permitted us to correlate $Ca_v3.1$ and $Ca_v3.3$ to the ''fast'' and ''slow'' thalamic LVA channels, respectively, provided a molecular substrate to the abstract concepts of ''fast'' and ''slow'' thalamic channels, and allowed one to be more specific in assigning a developmental role to the endogenous $Ca_v3.3$ and maybe $Ca_v3.2$ and signaling role to $Ca_v3.1$ T-channel $\alpha 1$ subunits.

Acknowledgment

We thank Dr. V. Naidenov for the invaluable technical assistance.

References

[1] Perez-Reyes E, Cribbs LL, Daud A, Lacerda AE, Barclay J, Williamson MP, et al. Molecular characterization of a neuronal low-voltage-activated T-type calcium channel. Nature 1998;391:896–900.
[2] Cribbs LL, Lee JH, Yang J, Satin J, Zhang Y, Daud A, et al. Cloning and characterization of alpha1H from human heart, a member of the T-type Ca^{2+} channel gene family. Circ Res 1998;83:103–9.
[3] Lee JH, Daud AN, Cribbs LL, Lacerda AE, Pereverzev A, Klockner U, et al. Cloning and expression of a novel member of the low voltage-activated T-type calcium channel family. J Neurosci 1999;19:1912–21.
[4] Perez-Reyes E. Three for T:molecular analysis of the low voltage-activated calcium channel family. Cell Mol Life Sci 1999;56:660–9.
[5] Akaike N, Kostyuk PG, Osipchuk YV. Dihydropyridine-sensitive low-threshold calcium channels in isolated rat hypothalamic neurones. J Physiol 1989;412:181–95.
[6] Heady TN, Gomora JC, Macdonald TL, Perez-Reyes E. Molecular pharmacology of T-type Ca^{2+} channels. Jpn J Pharmacol 2001;85:339–50.
[7] Tarasenko AN, Kostyuk PG, Ereminm AV, Isaev DS. Two types of low-voltage-activated Ca^{2+} channels in neurones of rat laterodorsal thalamic nucleus. J Physiol 1997;499:77–86.
[8] Zhuravleva SO, Kostyuk PG, Shuba YM. Divalent cation selectivity of the subtypes of low voltage-activated Ca^{2+} channels in thalamic neurons. Neuroreport 1999;10:651–65.
[9] Zhuravleva SO, Kostyuk PG, Shuba YM. Subtypes of low voltage-activated Ca^{2+} channels in laterodorsal thalamic neurons: possible localization and physiological roles. Pflugers Arch 2001;441:832–9.
[10] Dzhura IO, Naidenov VG, Lyubanova OP, Kostyuk PG, Shuba YM. Characterization of hypothalamic low-voltage-activated Ca channels based on their functional expression in Xenopus oocytes. Neuroscience 1996;70:729–38.
[11] Steriade M, Llinas RR. The functional states of the thalamus and the associated neuronal interplay. Physiol Rev 1988;68:649–742.
[12] Batuev AS. Higher integrative systems of the brain. New York, London, Paris, Monteux, Tokyo, Melbourne: Gordon and Breach Science Publishers; 1987. p. 34.
[13] Gomora JC, Daud AN, Weiergraber M, Perez-Reyes E. Block of cloned human T-type calcium channels by succinimide antiepileptic drugs. Mol Pharmacol 2001;60:1121–32.
[14] Takahashi K, Akaike N. Nicergoline inhibits T-type Ca^{2+} channels in rat isolated hippocampal CA1 pyramidal neurones. Br J Pharmacol 1990;100:705–10.
[15] Takahashi K, Akaike N. Calcium antagonist effects on low-threshold (T-type) calcium current in rat isolated hippocampal CA1 pyramidal neurons. J Pharmacol Exp Ther 1991;256:169–75.
[16] Ishibashi H, Murai Y, Akaike N. Effect of nilvadipine on the voltage-dependent Ca^{2+} channels in rat hippocampal CA1 pyramidal neurons. Brain Res 1998;813:121–7.
[17] Richard S, Diochot S, Nargeot J, Baldy-Moulinier M, Valmier J. Inhibition of T-type calcium currents by dihydropyridines in mouse embryonic dorsal root ganglion neurons. Neurosci Lett 1991;132:229–34.
[18] Romanin C, Seydl K, Glossmann H, Schindler H. The dihydropyridine niguldipine inhibits T-type Ca^{2+} currents in atrial myocytes. Pflugers Arch 1992;420:410–2.
[19] Stengel W, Jainz M, Andreas K. Different potencies of dihydropyridine derivatives in blocking T-type but not L-type Ca^{2+} channels in neuroblastoma-glioma hybrid cells. Eur J Pharmacol 1998;342:339–45.

[20] Triggle DJ. 1,4-Dihydropyridines as calcium channel ligands and privileged structures. Cell Mol Neurobiol 2003;23:293–303.
[21] Perchenet L, Benardeau A, Ertel EA. Pharmacological properties of $Ca_v3.2$, a low voltage-activated Ca^{2+} channel cloned from human heart. Naunyn Schmiedebergs Arch Pharmacol 2000;361:590–9.
[22] Kumar PP, Stotz SC, Paramashivappa R, Beedle AM, Zamponi GW, Rao AS. Synthesis and evaluation of a new class of nifedipine analogs with T-type calcium channel blocking activity. Mol Pharmacol 2002;61:649–58.
[23] Fox AP, Nowycky MC, Tsien RW. Single-channel recordings of three types of calcium channels in chick sensory neurones. J Physiol 1987; 394:173–200.
[24] Talley EM, Cribbs LL, Lee JH, Daud A, Perez-Reyes E, Bayliss DA. Differential distribution of three members of a gene family encoding low voltage-activated (T-type) calcium channels. J Neurosci 1999;19:1895–911.
[25] Craig PJ, Beattie RE, Folly EA, Banerjee MD, Reeves MB, Priestley JV, et al. Distribution of the voltage-dependent calcium channel alpha1G subunit mRNA and protein throughout the mature rat brain. Eur J Neurosci 1999;11:2949–64.
[26] Hockerman GH, Peterson BZ, Sharp E, Tanada TN, Scheuer T, Catterall WA. Construction of a high-affinity receptor site for dihydropyridine agonists and antagonists by single amino acid substitutions in a non-L-type Ca^{2+} channel. Proc Natl Acad Sci USA 1997;94:14906–11.
[27] Sinnegger MJ, Wang Z, Grabner M, Hering S, Striessnig J, Glossmann H, et al. Nine L-type amino acid residues confer full 1,4-dihydropyridine sensitivity to the neuronal calcium channel alpha1A subunit. Role of L-type Met1188. J Biol Chem 1997;272:27686–93.
[28] Ito H, Klugbauer N, Hofmann F. Transfer of the high affinity dihydropyridine sensitivity from L-type to non-L-type calcium channel. Mol Pharmacol 1997;52:735–40.
[29] Furukawa T, Yamakawa T, Midera T, Sagawa T, Mori Y, Nukada T. Selectivities of dihydropyridine derivatives in blocking Ca^{2+} channel subtypes expressed in Xenopus oocytes. J Pharmacol Exp Ther 1999;291:464–73.
[30] Talley EM, Solorzano G, Depaulis A, Perez-Reyes E, Bayliss DA. Low-voltage-activated calcium channel subunit expression in a genetic model of absence epilepsy in the rat. Mol Brain Res 2000;75:159–65.
[31] Perez-Reyes E. Molecular physiology of low-voltage-activated T-type calcium channels. Physiol Rev 2003;83:117–61.
[32] Soong TW, Stea A, Hodson CD, Dubel SJ, Vincent SR, Snutch TP. Structure and functional expression of a member of the low voltage-activated calcium channel family. Science 1993;260:1133–6.
[33] Yokoyama CT, Westenbroek RE, Hell JW, Soong TW, Snutch TP, Catterall WA. Biochemical properties and subcellular distribution of the neuronal class E calcium channel alpha 1 subunit. J Neurosci 1995;15:6419–32.